Aytore *et al. Earth, Planets and Space* (2016) 68:139
DOI 10.1186/s40623-016-0508-z

Earth, Planets and Space

FRONTIER LETTER

Open Access

Assessment of tsunami resilience of Haydarpaşa Port in the Sea of Marmara by high-resolution numerical modeling

Betul Aytore[1], Ahmet Cevdet Yalciner[1*], Andrey Zaytsev[2,3], Zeynep Ceren Cankaya[4] and Mehmet Lütfi Suzen[4]

Abstract

Turkey is highly prone to earthquakes because of active fault zones in the region. The Marmara region located at the western extension of the North Anatolian Fault Zone (NAFZ) is one of the most tectonically active zones in Turkey. Numerous catastrophic events such as earthquakes or earthquake/landslide-induced tsunamis have occurred in the Marmara Sea basin. According to studies on the past tsunami records, the Marmara coasts have been hit by 35 different tsunami events in the last 2000 years. The recent occurrences of catastrophic tsunamis in the world's oceans have also raised awareness about tsunamis that might take place around the Marmara coasts. Similarly, comprehensive studies on tsunamis, such as preparation of tsunami databases, tsunami hazard analysis and assessments, risk evaluations for the potential tsunami-prone regions, and establishing warning systems have accelerated. However, a complete tsunami inundation analysis in high resolution will provide a better understanding of the effects of tsunamis on a specific critical structure located in the Marmara Sea. Ports are one of those critical structures that are susceptible to marine disasters. Resilience of ports and harbors against tsunamis are essential for proper, efficient, and successful rescue operations to reduce loss of life and property. Considering this, high-resolution simulations have been carried out in the Marmara Sea by focusing on Haydarpaşa Port of the megacity Istanbul. In the first stage of simulations, the most critical tsunami sources possibly effective for Haydarpaşa Port were inputted, and the computed tsunami parameters at the port were compared to determine the most critical tsunami scenario. In the second stage of simulations, the nested domains from 90 m gird size to 10 m grid size (in the port region) were used, and the most critical tsunami scenario was modeled. In the third stage of simulations, the topography of the port and its regions were used in the two nested domains in 3-m and 1-m resolutions and the water elevations computed from the previous simulations were inputted from the border of the large domain. A tsunami numerical code, NAMI DANCE, was used in the simulations. The tsunami parameters in the highest resolution were computed in and around the port. The effect of the data resolution on the computed results has been presented. The performance of the port structures and possible effects of tsunami on port operations have been discussed. Since the harbor protection structures have not been designed to withstand tsunamis, the breakwaters' stability becomes one of the major concerns for less agitation and inundation under tsunami in Haydarpaşa Port for resilience. The flow depth, momentum fluxes, and current pattern are the other concerns that cause unexpected circulations and uncontrolled movements of objects on land and vessels in the sea.

Keywords: Tsunami, Resilience, Port, Marmara Sea, Simulation, Modeling

*Correspondence: yalciner@metu.edu.tr
[1] Department of Civil Engineering, Ocean Engineering Research Center, METU, 06800 Ankara, Turkey
Full list of author information is available at the end of the article

Background

The Sea of Marmara is located on the western extension of the North Anatolian Fault Zone (NAFZ). It has three branches, two of which extend in the Marmara Sea. NAFZ is one of the most important active faults with strike-slip characteristics, which are not likely to generate tsunami. However, in the light of tsunami catalogs based on historical documents, it is possible to say that Marmara Sea has tsunamigenic potential. Based on the latest tsunami catalog on tsunamis triggered around the Turkish coasts, which was prepared by Altinok et al. (2011), 35 tsunami events out of 134 from the seventeenth century BC to the recent 1999 Marmara event have occurred in the Sea of Marmara. Since numerous catastrophic tsunami events have occurred in the Marmara Sea basin and may continue to occur in the future, various studies were conducted on tsunamis in the Sea of Marmara by Yalciner et al. (2002); Altinok et al. (2011); Papadopoulos et al. (2014); Hébert et al. (2005); Insel (2009); Aydin (2014); Ayca (2012); Ozel et al. (2011); Ozdemir (2014); Aytöre et al. (2013, 2014); and Aytöre (2015).

The megacity Istanbul utilized the northern coast of the Marmara Sea. It is one of the most populated cities in the world and has a great importance owing to its strategic location on the Bosporus Strait and its invaluable historical assets, more than 300,000 years old (Istanbul Metropolitan Municipality 2009). The transcontinental city also plays a crucial role as an industrial and commercial center in Turkey. Corresponding to the economic significance of Istanbul, the city possesses several commercial ports and one of those ports is Haydarpaşa Port. The port is the oldest and the largest container port in the Marmara region and third largest in the nation. The port and its environments are placed in between two counties, which are the two of the most populous counties among the 32, Kadikoy and Uskudar in the Anatolian side of Istanbul (Istanbul Metropolitan Municipality 2009). The location and general view of the port are shown in Fig. 1. One of the main docks in the Asian side for domestic maritime transportation, Kadikoy Ferry Terminal, and a historical train station constructed in 1908 are also located in the selected study area.

Water-related disasters, particularly tsunamis, should be carefully investigated since many of the historical, industrial, and commercial structures are situated near the coastal areas of Istanbul. These can cause excessive damage especially on the ports as a consequence of their vulnerability against such forces and may in turn cause not just loss of life, but also loss of property resulting in negative economic effect on the region and even the country. Hence, the Haydarpaşa Port area was selected for the case study of tsunami assessment. Guler et al. (2015) studied the performance of Haydarpaşa breakwaters under the attack of solitary-type long waves and continuous overflow by physical model experiments. In this study, the port was selected for a case study since the trapped tsunami waves inside the ports or enclosed basins lead to strong currents, tend to show resonant amplifications for hours, and damage the port components and structures. Hence, after the tsunami, the port

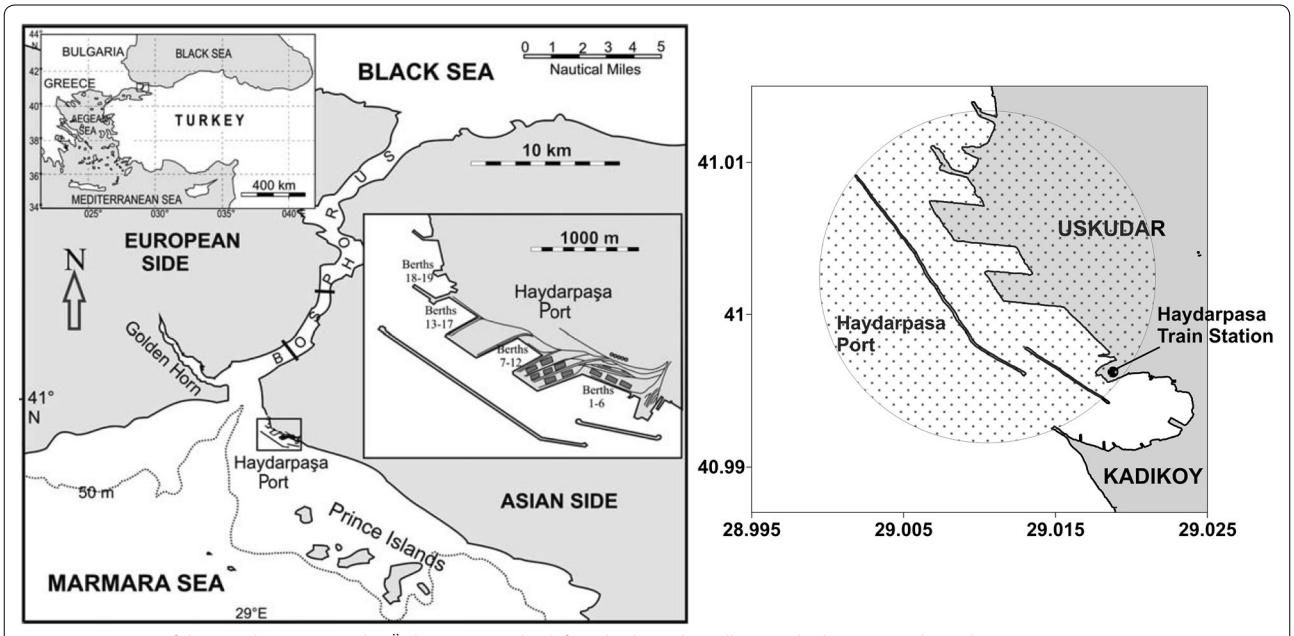

Fig. 1 Location of the Haydarpasa Port (by Ünlü 2007) on the *left* and selected smallest study domain on the *right*

operations are interrupted. Assessment of such damaging effects of tsunamis inside the harbors is important for the management of post-disaster operations.

Bathymetric and topographical maps

The bathymetric data for high-resolution modeling were acquired from General Bathymetric Chart of the Oceans (GEBCO 2016) of the British Oceanographic Data Centre (spatial resolution of 30 arc seconds). The dataset obtained from the navigational charts was added to improve the bathymetric data in the shallow zone. Besides, the images from Google Earth were used to define a better shoreline and location of the breakwaters in the selected domain. The cross section of breakwaters of Haydarpaşa Port was acquired from the technical drawings used in the construction of the breakwaters.

The topographical data are purchased from the Directorate of Cartography under the Department of Housing and Urban Development of Istanbul Metropolitan Municipality (IMM). The data purchased from IMM, shown in Fig. 2, have two basic parts: raster data (digital elevation models) and vector data (points, lines, and polygonal features) that cover all the counties of Istanbul. The resolutions of DEMs and vector data are 5 m and 1 m, respectively. While the polygonal vector data cover all types of structures that exist in the selected region (religious buildings, greenhouses, commercial buildings, schools, load control platform, residential buildings, etc.), the line vector data cover the line-shaped structures (roads, retaining wall, dock, railway and roadway, walls, etc.). The available point vector data are not that crucial since point data mainly cover point structures such as lighting post, bush, and sculpture, which are not as effective as polygonal objects when it comes to their resistance against tsunami forces.

Based on the selected study domains for numerical modeling, topographical and bathymetric data were eliminated and processed. A series of simulations performed in this study was categorized into two different model applications: Model 1 was used for the determination of the critical submarine source near the port and Model 2 was used for high-resolution numerical modeling. Two different models were created since decreasing the grid size to a very small value to cover a large area such as the Marmara Sea results in a very large size of matrix, which causes a longer simulation duration.

Tsunami analyses using the first model were performed in the nested study domains B, C, and D. The grid size of the largest domain named Domain B was chosen as 90 m. According to the principle of nested analyses in NAMI DANCE, the boundary of the smaller domain should involve the previous larger domain and the smaller domain should have one-third the grid size of the previous larger domain. Because of this principle, the grid sizes of Domains C and D were 30 m and 10 m, respectively. For the second model's analyses (high-resolution modeling), the nested study Domains C and D that were characterized by grid size of 3 m and 1 m, respectively, were used. The general view of the nested study domains of these two models is shown in Fig. 3. Table 1 also summarizes the nested study domains of Model 1 and Model 2 with their boundary coordinates and grid sizes.

Tsunami source selection and related rupture parameters

There are six critical active faults (OYO and IMM 2007 and Ayca 2012) in the Sea of Marmara according to the previous studies: Prince's Islands Strike Slip (PI) fault, Prince's Islands Normal (PIN) fault, Ganos Strike Slip (GA) fault, Yalova Normal (YAN) fault, Central Marmara Normal (CMN) fault, and the combination of Prince's Islands and Ganos Strike Slip (PI + GA) faults. According to the presented results by Ayca (2012), it has been revealed that the tsunami generated at YAN, PIN, and

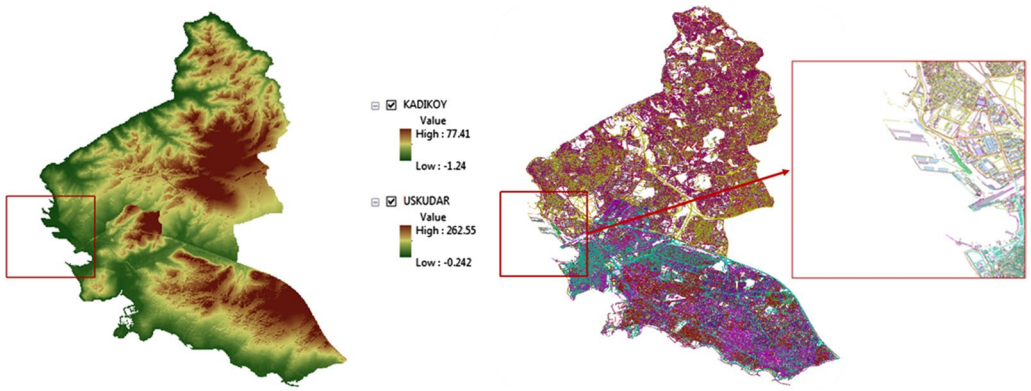

Fig. 2 View of available DEMs on the *left* and vector data on the *right* for both Uskudar and Kadikoy region with indicating the smallest selected domain for the study

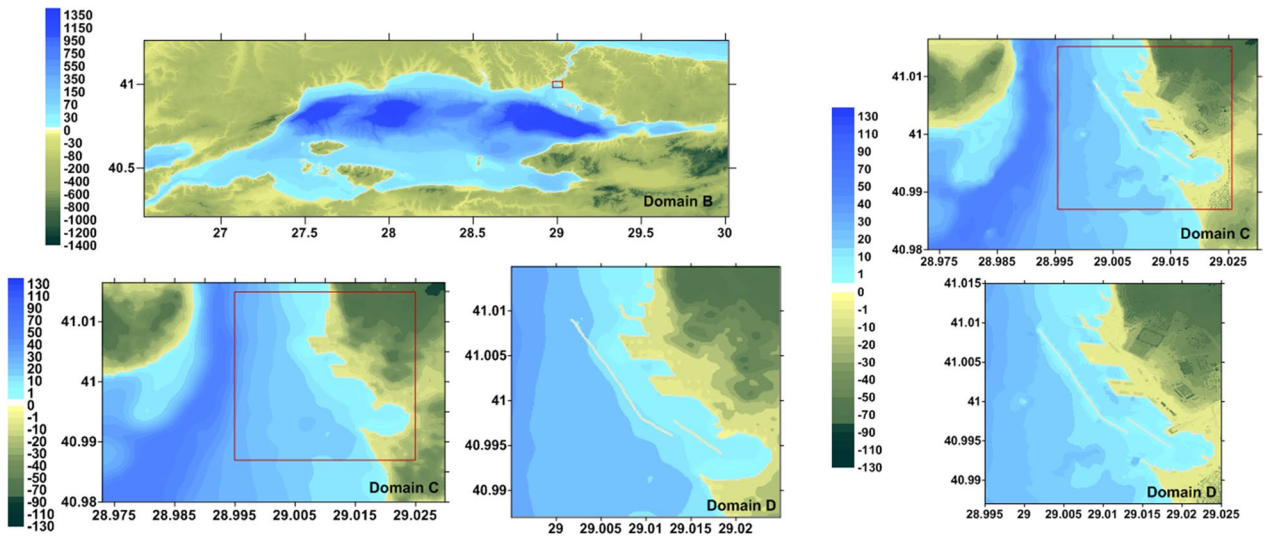

Fig. 3 Nested study *Domains B*, *C*, and *D* used in the simulation of Model 1 on the *left* **a** and nested study *Domains C* and *D* used in the simulation of Model 2 on the *right* **b**. The *red rectangles* inside the larger domains indicate the location of next smaller domain inside (scales are in meters)

Table 1 Summary of the grid size and boundaries of study domains of Models 1 and 2

Domain name	Grid size (m)	Coordinates of the domains
Model 1		
B	90	40.21°–41.26° N 26.542°–30.02° E
C	30	40.98°–41.0165° N 28.973°–29.030° E
D	10	40.987°– 41.015° N 28.995°–29.025° E
Model 2		
C	3	40.98°–41.0165° N 28.973°–29.030° E
D	1	40.987°–41.015° N 28.995°–29.025° E

CMN increases the water level, flow depth, and current velocities near Haydarpaşa Port, unlike tsunamis originating elsewhere. Thus, these segmented faults were selected for comparison in the new simulations for Haydarpaşa Port, and the most critical one was used in the high-resolution simulation as the final source.

The rupture parameters of each segment for the selected faults YAN, PIN, and CMN are shown in Fig. 4. Considering the uncertainties, the slip displacements were estimated to be 5 m, as suggested by Ayca (2012). Unlike the OYO and IMM (2007) report, in which the vertical displacements were estimated to be around 3.67 m for normal segments, Ayca (2012) explained the proposed vertical displacement change by citing that the vertical displacement in the 2011 Great East Japan Tsunami was almost two times more than expected. Using a 5-m slip instead of 3.67-m slip makes the tsunami height 1.36 times larger. Therefore, the results obtained in this study are conservative in comparison with the well-accepted tsunami source characteristics. The tsunami sources were computed using Okada (1985). The simulation results of YAN, PIN, and CMN simulations are shown in Fig. 4.

The high-resolution modeling with the grid size in order of meters required two-stage simulations. In the first stage, the rupture parameters were inputted to the model using three nested domains from the whole Marmara Sea (90 m gird size) to the port area (10 m grid size). While computing the tsunami parameters in the port area for comparison of the tsunami effects of each source, the time series of water surface fluctuations at the border of Domain C (at the numerical gauges along the border) are also computed and stored for the fine-grid near-field simulations. In these simulations, the tsunami wave (time history of water level) was inputted from the border of the domain. Since the tsunami source does not extend in Domain C, the input from the border in the simulations for the small domain near the shore was possible, which also enabled the high-resolution analysis (1 m grid size) of Haydarpaşa Port. The time series of water surface fluctuations to be used as the border source were selected among the performed nested domain simulations of YAN, PIN, and CMN. The numerical gauges placed on the border of Domain C are shown in Fig. 5, and the maximum positive and negative water levels obtained by the end of each simulation are presented in Table 2.

Based on the distribution of the maximum water level (Table 3), it was clear that CMN is not a critical fault

	Lon. (°)	Lat. (°)	Depth (m)	Strike (°)	Dip (°)	Rake (°)	Length (m)	Width (m)	Vertical Disp. (m)
YAN	29.47103	40.72115	1978	257.96	70	195	7058	17027	5
	29.38946	40.70850	1960	261.14	70	195	6873	17027	5
	29.30920	40.69851	1823	260.98	70	195	10952	17027	5
	29.18143	40.68121	1681	262.35	70	270	4448	17027	5
	29.12936	40.67650	1557	273.96	70	270	4562	17027	5
	29.07651	40.67891	1252	283.78	70	270	10021	17027	5
	28.96007	40.69843	1219	294.84	70	270	3154	17027	5
	28.96202	40.71005	1178	284.90	70	270	14043	17027	5
PIN	29.12942	40.75691	744	108.15	70	270	8753	17027	5
	29.06928	40.78610	740	123.15	70	270	6024	17027	5
	28.99465	40.81653	779	118.85	70	270	7148	17027	5
	28.90432	40.87251	1210	129.90	70	270	9834	17027	5
CMN	28.19394	40.6126	1924	276.59	70	270	9505	17027	5
	28.08215	40.6206	1922	279.18	70	270	7069	17027	5
	27.99943	40.6294	1917	299.07	70	270	10705	17027	5
	27.88744	40.6742	1598	283.92	70	270	7850	17027	5
	27.79683	40.6895	1637	291.38	70	270	7269	17027	5

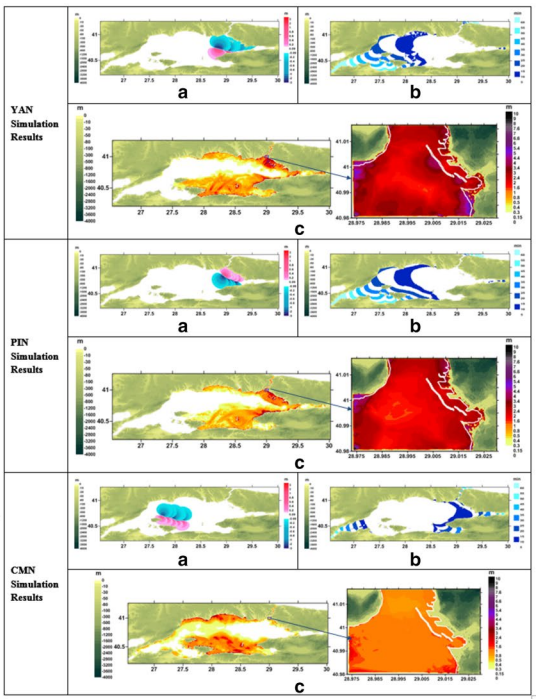

Fig. 4 Estimated rupture parameters for each segment of each source YAN, PIN, and CMN (*left*) and initial sea state in Domain B **a**, distribution of arrival time of first wave in Domain B **b**, distribution of maximum water surface elevation in Domain B and Domain C **c** after YAN, PIN, and CMN simulations (depth refers to focal depth)

for Haydarpaşa Port when compared with the results of case studies of YAN and PIN. The maximum wave amplitudes were around 1–2 m in case of tsunamis originating at CMN, whereas those originating at YAN and PIN were around 2–4 m (Table 2). Therefore, the CMN fault will not be considered as a critical source for Haydarpaşa henceforth in this study.

On the other hand, whether YAN or PIN is the critical fault for the region and which one should be used as a source in the series of tsunami analysis to be performed in NAMI DANCE were difficult to determine. Thus, the water level fluctuation at some of the previously determined border gauges after the YAN and PIN simulations were compared, and the results are shown in Fig. 5.

When all the computed tsunami time series were carefully examined, it was determined that even the computed time series of the tsunamis with PIN and YAN sources were quite close to each other. The YAN source, with a leading depression wave propagating toward Haydarpaşa Port, was more effective than the PIN source in the study area. Thus, the YAN source was used as input for the near-field high-resolution simulations for the assessment of tsunami resilience at Haydarpaşa Port.

Among different water level fluctuations presented, "cborder9" results obtained from the YAN simulations were selected to be used as the border source in the high-resolution simulation. The reasons for this selection are as follows: "cborder3" and "cborder4" are located far from the port area and right across to the breakwaters, thereby blocking the tsunami waves and causing less fluctuations inside the port; "cborder5" is located at the corner of the selected domain, which is susceptible to instabilities and leads to lower reliability on the data as compared to other gauges; among the remaining gauges, higher water level changes were observed at "cborder9."

Simulation results

The numerical code, NAMI DANCE, was used in the simulations. The code solves nonlinear forms of shallow-water relations with friction and computes the principal tsunami hydrodynamic parameters, namely water surface elevation, current velocities and their directions, flow depth, and Froude number of the selected output time intervals throughout the study domain in either a Cartesian or spherical coordinate system. Moreover, the model can calculate using either the static source data created as an initial wave or dynamic source data (time history of water surface fluctuation) inputted as a line from an arbitrary location. The improved code version was applied here, calculating the land inundation more precisely, without instability by using very fine bathymetric/topographical data (NAMI DANCE 2016). The duration

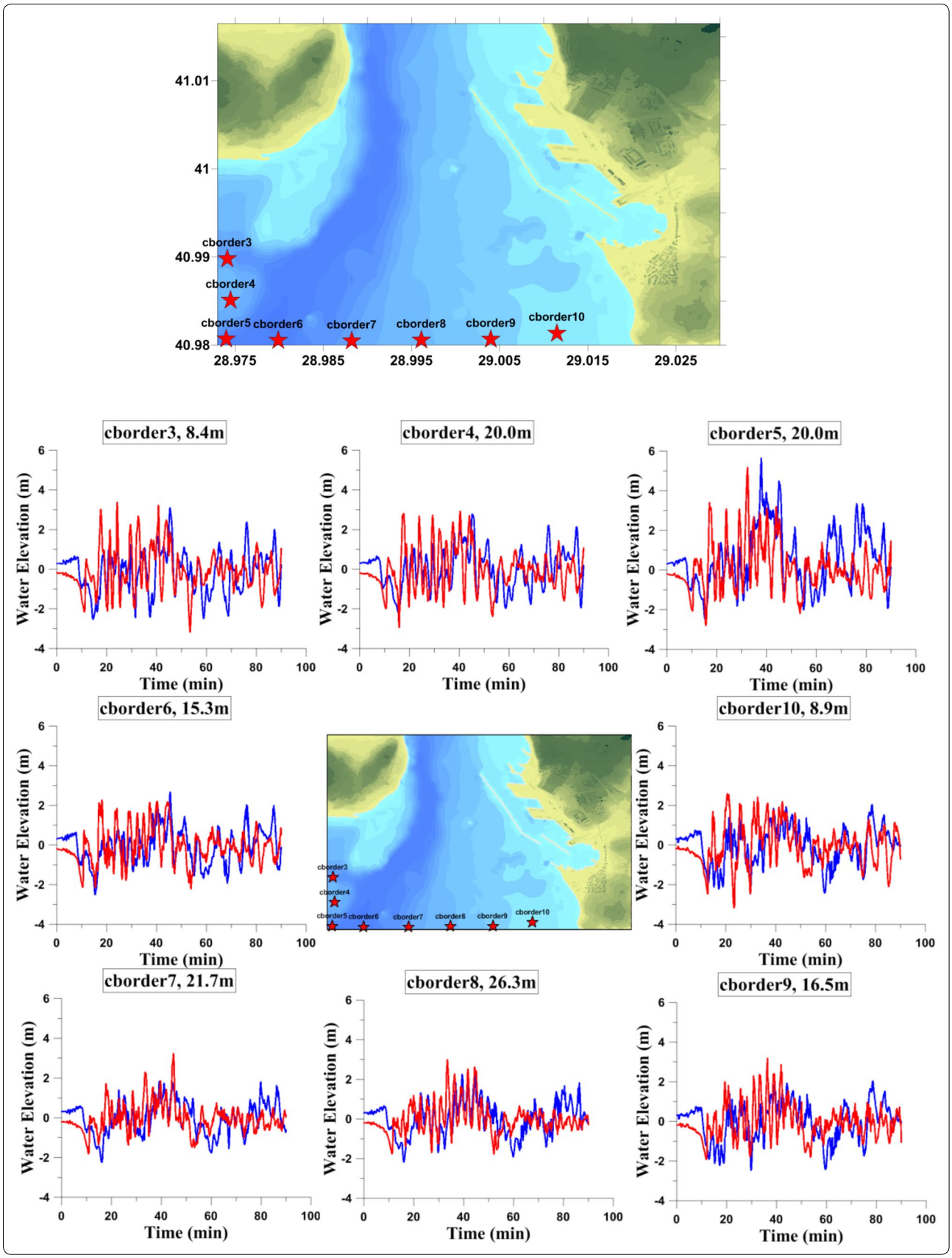
41.01
41
40.99
40.98
cborder3
cborder4
cborder5
cborder6
cborder7
cborder8
cborder9
cborder10
28.975
28.985
28.995
29.005
29.015
29.025
cborder3, 8.4m
cborder4, 20.0m
cborder5, 20.0m
cborder6, 15.3m
cborder10, 8.9m
cborder7, 21.7m
cborder8, 26.3m
cborder9, 16.5m
Water Elevation (m)
Time (min)

(See figure on previous page.)
Fig. 5 Border gauges placed in Domain C to determine the border source (*top*) and comparison of water level fluctuations at border gauges obtained after YAN and PIN simulations (in the figure, *red lines* represent YAN simulation results and *blue lines* represent PIN simulation results, and time starts with the earthquake)

of the simulations was 90 min, and the selected time step was 0.005 s, which satisfies the CFL condition. Since the largest tsunami waves hit the area in the first 45 min, 90 min of propagation was considered to obtain reliable results, including wave reflections. The simulation duration also included the arrival of the wave reflected from the southern coast of the Marmara Sea. In addition, the friction coefficient was taken as zero.

The tsunami parameters of the high-resolution model were computed near the shorelines in Domain D, and the results are presented in Fig. 6. The arrival time of the initial and maximum tsunami waves and the maximum positive and negative wave amplitudes at the selected gauges (see Fig. 6) are also listed in Table 3. In addition, the time histories of the current velocity at some selected gauge points are shown in Fig. 6. As shown in the figure, the current velocities at the selected gauge points were in the range of 2–4 m/s, except the gauges "p55" and "p8," where the maximum current velocity reached 7–8 m/s. The computed time histories at the numerical gauges on the breakwater and land show that the horizontal viscosity in the computation was relatively small.

Tsunami risk assessment of Haydarpaşa Port

Figure 7 shows the final aerial view of Haydarpaşa Port prepared by NAMI DANCE with the distribution of maximum flow depths on land.

According to Fig. 6 and Table 3, it was seen that the initial tsunami wave reached the port area in 5 min after

Table 2 Maximum positive and negative wave amplitudes observed at each the numerical gauges along the border as the result of simulations by inputting YAN, PIN, and CMN sources

Border gauge	Depth	YAN		PIN		CMN	
		Max. (+)ve amp. (m)	Max. (−)ve amp. (m)	Max. (+)ve wave amp. (m)	Max. (−)ve wave amp. (m)	Max. (+)ve wave amp. (m)	Max. (−)ve wave amp. (m)
cborder3	8.4	3.4	−3.2	3.1	−2.5	1.9	−0.9
cborder4	20.0	2.9	−2.9	2.8	−2.2	1.5	−0.8
cborder5	20.0	5.2	−2.8	5.6	−2.5	1.8	−0.7
cborder6	15.3	2.3	−2.2	2.7	−2.5	1.7	−0.8
cborder7	21.7	3.2	−1.8	1.8	−2.2	1.4	−0.6
cborder8	26.3	3.0	−1.8	2.3	−2.2	1.1	−0.6
cborder9	16.5	3.2	−1.9	2.9	−2.1	1.2	−0.7
cborder10	8.9	2.6	−3.2	2.0	−2.5	1.5	−0.8

Table 3 Maximum positive and negative wave amplitudes and arrival time of initial and maximum wave at selected numerical gauge points with their water depths and coordinates

Name of gauge Pt.	Depth (m)	Longitude (°)	Latitude (°)	Arrival time of initial wave (min)	Arrival time of max. wave (min)	Max. (+)ve wave amp. (m)	Max. (−)ve wave amp. (m)
p2	4.2	29.0204	40.9917	3	20	3.2	−2.6
p8	4.5	29.0197	40.9954	3	37	3.2	−2.3
p13	7.2	29.0171	40.9982	3	17	1.8	−3.6
p24	8.1	29.0124	41.0035	3	23	3.0	−4.1
p35	8.8	29.0094	41.0078	3	22	4.1	−5.3
p50	12.1	29.0063	41.0058	3	22	2.7	−3.6
p52	11.6	29.009	41.0013	3	38	2.1	−3.3
p55	5.3	29.0164	40.9966	3	39	1.9	−3.8

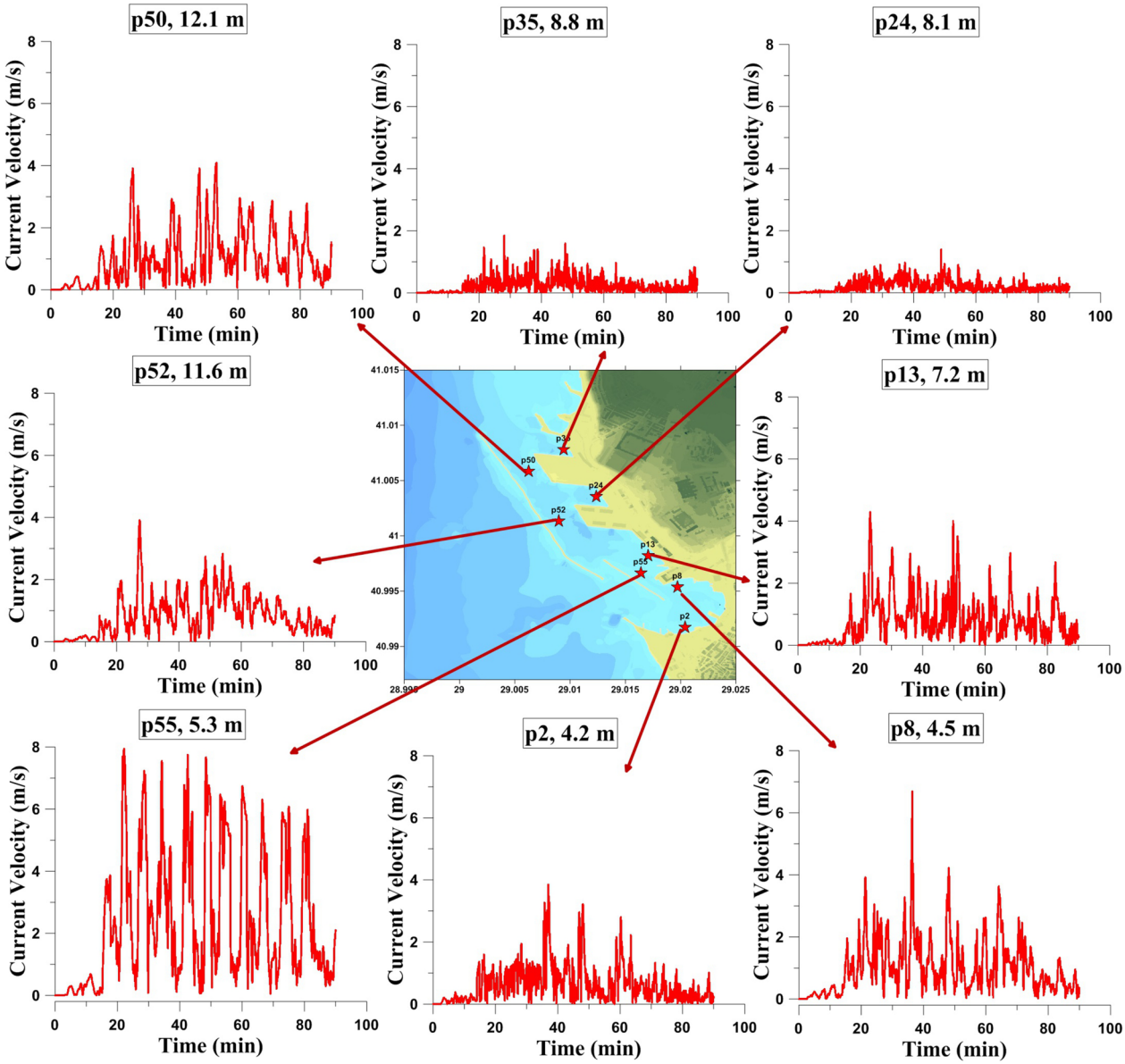

Fig. 6 Time histories of current velocity at some selected numerical gauge locations

the earthquake. After 20 min, the maximum tsunami wave was observed in the port area. Considering the run-up plot shown in Fig. 8, the maximum run-up values changed between 4.5 m and 6 m. The inundation distance was computed to be 340 m on one of the docks at the port and in the Kadikoy Peninsula to the southeast of the port. It is also important to state here that the computed values in Table 3 do not cover the possible change in water level in cases of long-term and short-term rise due to wind, wave, and barometric effects (setup) during the storm and surge conditions that occur during tsunami in general. The large ships moored in the harbor can resist the water motion and influence the inundation. In the simulations, the existence of large container ships was excluded in order to be conservative.

The conclusions based on the obtained results are as follows:

1. The two breakwaters in the region reduce the effect of tsunami waves on the coast and port environments. However, wave overtopping was observed on the breakwaters after a while. It is possible that this

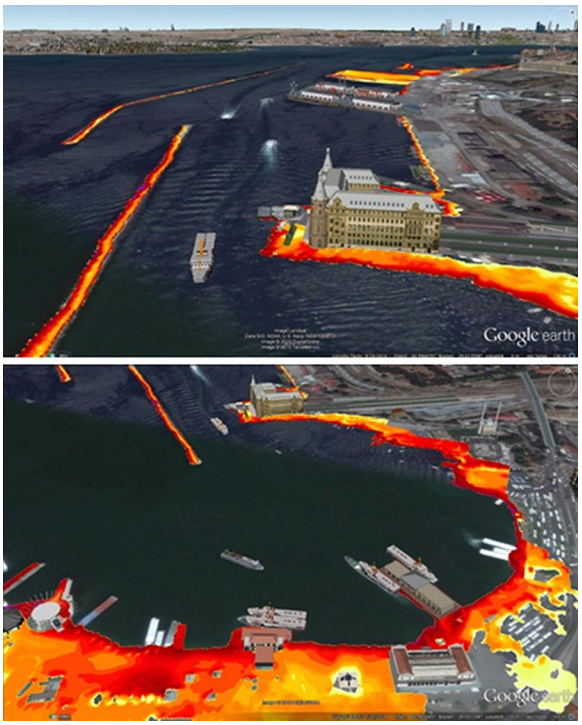

Fig. 7 3D view of tsunami inundation at Haydarpaşa and Kadikoy region

overtopping discharge will damage the breakwaters and affect their stability. This may lead to an increase in tsunami inundation extent presented in this study.

2. Higher run-up values were observed at the corners of the inner (rhombohedron-shaped) basin. They trap water inside and cause additional water level increase inside the inner basins.
3. The current velocities exceeded 6 m/s at some locations, especially in the region bounded by two parallel breakwaters and at the entrance of the circular basin. Current velocities were also high around the breakwaters, which may have caused scouring at the toe of the coastal structures.
4. The simulation shows that the water flowed parallel to the breakwaters during the tsunami. The flow of water parallel to rubble-mound breakwater may have caused scouring at the toe of the slope and instability of the breakwater.
5. Some structures located the near shoreline may have been partially damaged as a result of the impact of tsunami waves.
6. Damages and dragging of floating bodies such as cargo vessels or ferries due to strong currents and water level rise at the port should be expected. Similarly, they can damage some structures near the coastline.
7. Since this is the largest container port in the Marmara region, a great number of containers are usually present at various locations around it. High current velocities were especially observed in the rhombohedron-shaped basin in the port. Thus, the containers in this area can also be floated and dragged.
8. The selected study area is an urbanized area and hosts many structures in the coastal zone. Current velocities might increase in between the solid structures because of channel effect. For example, two storage buildings of the port are located in the rhombohedron-shaped basin, parallel to each other, as shown in Fig. 9. Two different profiles were considered for the examination of the channel effect. One of the profiles was located adjacent to the storage buildings, and the other one is located along the storage buildings. As shown in Fig. 9, the current velocities are higher between the storage buildings as expected.
9. Even if the simulation results do not show wave penetration in the railway lines at Haydarpaşa Train Station, it is also recommended that protective structures (walls, dikes) against tsunami inundation should be installed to prevent unexpected damages on transportation elements at the station (see Fig. 7).
10. Although this study focused on Haydarpaşa Port, the arc-shaped bay to the south of the port near Kadikoy is also another important area. Because there are inter-city passenger and ferry terminals, it serves as one of the most important business districts of Istanbul at Kadikoy. This area is highly inundated according to the simulation results. Thus, tsunami hazard analysis, specifically for the Kadikoy district, is also necessary (see Fig. 9).

In brief, it is also safe to say that a tsunami will negatively affect this urbanized area and its economic and social aspects.

Discussion and conclusions

Based on the simulation results of the high-resolution numerical modeling for Haydarpaşa Port, the water inside the port will be agitated and water flow parallel to the breakwaters will affect major port operations. This behavior will cause amplification of the water level and current velocities inside the port. Damages and dragging of floating bodies due to strong currents and water level rise at the port should also be expected.

During this study, the friction effect on the calculated tsunami parameters was ignored. It has been suggested for future studies to investigate the effect of friction on the calculated tsunami parameters by defining proper Manning's coefficient scheme for the entire topography.

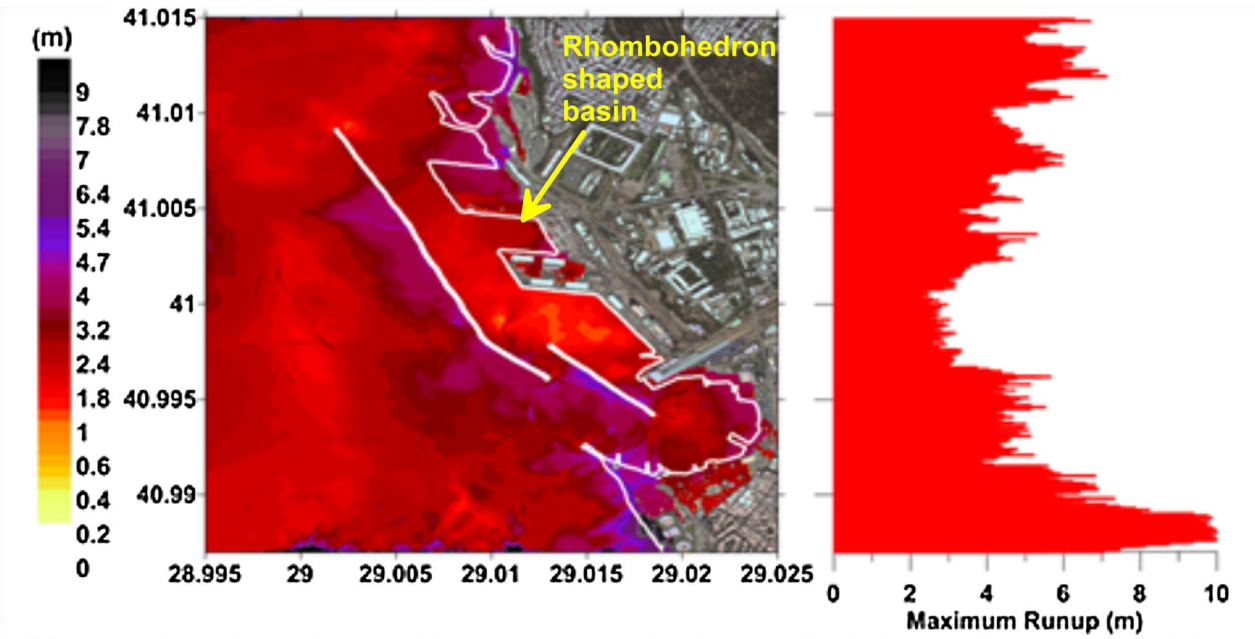

Distribution of maximum (+)ve wave amplitudes on the left and the run-up heights (maximum near shore (+)ve tsunami amplitudes) on the right at land in Domain D during the entire tsunami simulation

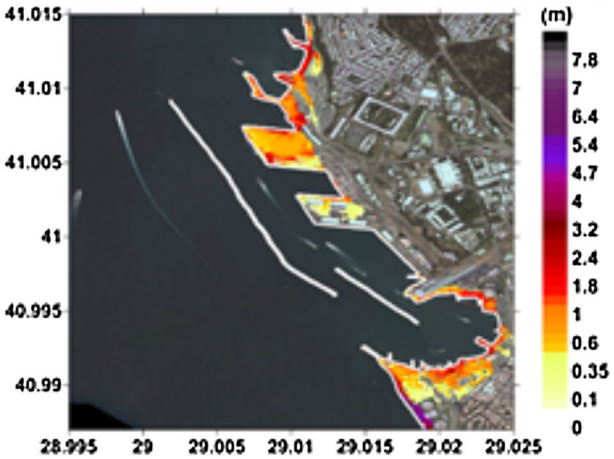

Distribution of maximum flow depth in Domain D

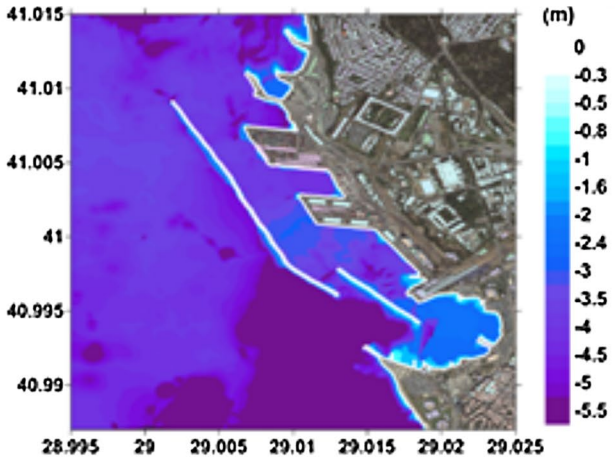

Distribution of maximum (-)ve wave amplitudes in Domain D

The maximum near shore positive tsunami amplitude : 6.5 m
The minimum near shore negative tsunami amplitude : -6.5 m
The maximum flow depth : 4.8 m
Maximum inundation distance : 340m

Fig. 8 Computed tsunami parameters of high-resolution model

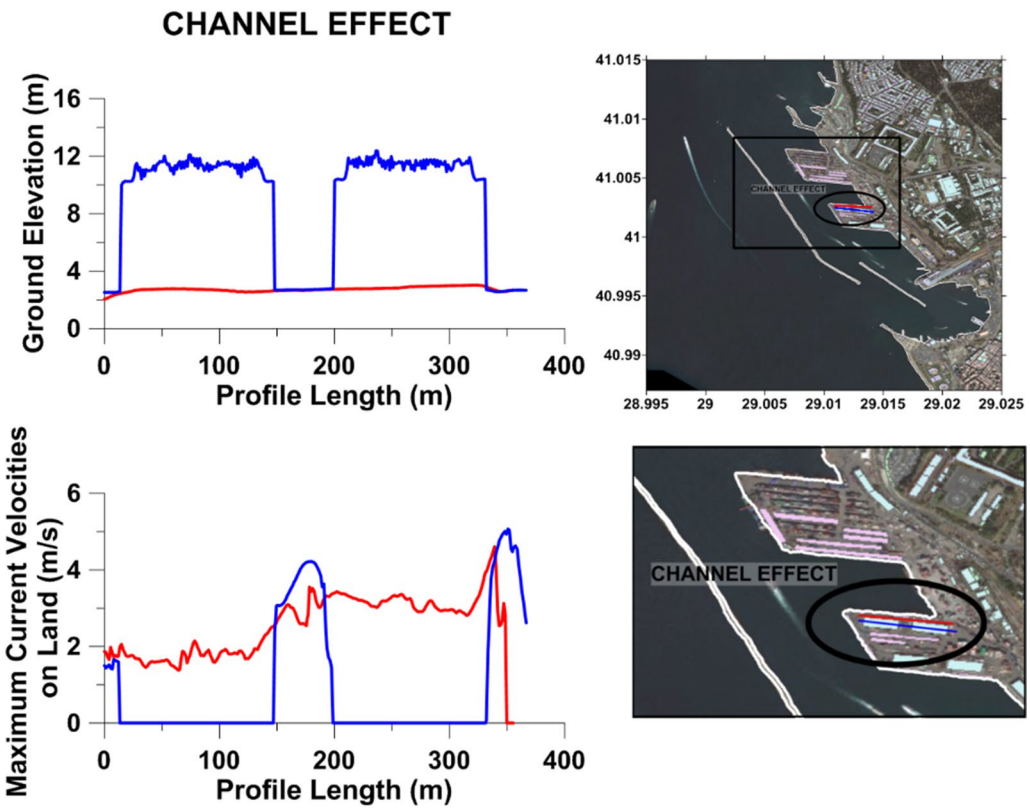

Fig. 9 Change in maximum current velocity according to ground elevation along two different sections. *Blue lines* represent cross-sectional change in ground elevation and of maximum current velocity along the *blue line* at *right* crossing two storage buildings. *Red lines* represent cross-sectional change in ground elevation and of maximum current velocity along the *red line* at *right* crossing the area without buildings

The vegetation of the selected area should also be considered because presence of vegetation may prevent the tsunami waves to penetrate to the inner zones, and thus, change the inundation extent.

Resilience of Haydarpaşa Port after a disaster is important for Istanbul. The port operations should not be affected after a tsunami. One of the main requirements to enhance the resilience of Haydarpaşa Port is to prevent the damage of port components, which can be achieved by less amplification inside the port and less inundation at the area of cargo handling and storage facilities. Since one of the main causes of amplification is the parallel reflective berths at the rhombohedron-shaped basin, the reflective surfaces in the port must be maintained to reduce the wave amplification.

In addition, the vulnerability analysis of the port and its surrounding area can be performed in future studies, and the high-resolution map of this region is available with the detailed structural information.

Authors' contributions

BA has compiled and processed the data, carried out the simulations, analyzed the simulation results, converted them to graphical representations, and conducted necessary discussions/comparisons in her MSc thesis. She also interpreted the simulation results and made necessary discussions and conclusions. ACY developed the tsunami numerical model with AZ, and monitored the simulations and supervised BA thesis work at all stages, from the beginning to the defense. He also contributed to the interpretation of the simulation results and necessary discussions and conclusions. AZ developed the tsunami numerical code NAMI DANCE with ACY, and he inserted the necessary output parameters to the code for the paper. He also contributed to the interpretation of the simulation results, discussions, and conclusions. Z\CC and LS dedicated their expertise to the assessment and quality of the compiled high-resolution topographic data considering the buildings and all other structures at Haydarpasa and its surroundings. They also contributed to the interpretation of the simulation results, discussions, and conclusions. All authors read and approved the final manuscript.

Author details

[1] Department of Civil Engineering, Ocean Engineering Research Center, METU, 06800 Ankara, Turkey. [2] Special Research Bureau for Automation of Marine Researches, Russian Academy of Sciences, 693013 Sakhalinsk, Russia. [3] Nizhny Novgorod State Technical University, 24 Minin Street, Nizhny Novgorod, Russia. [4] Department of Geological Engineering, Remote Sensing and Geographical Information Systems Laboratory, METU, 06800 Ankara, Turkey.

Acknowledgements

This study was partly supported by Japan–Turkey Joint Research Project by JICA on earthquakes and tsunamis in the Marmara region by MarDim SATREPS, EC project ASTARTE-Assessment, Strategy And Risk Reduction for Tsunamis in Europe - FP7-ENV2013 6.4-3, Grant 603839, UDAP-Ç-12-14 project granted by Disaster Emergency Management Presidency of Turkey (AFAD), and RAPSODI (CONCERT_Dis-021) project in the framework of CONCERT-Japan, Research

and Innovation Joint Call for connecting and cooperating European Research and Technology Development with Japan and TUBITAK 113M556 and 108Y227 Projects.

Competing interests
The authors declare that they have no competing interests.

Received: 27 October 2015 Accepted: 6 July 2016
Published online: 02 August 2016

References

Altinok Y, Alpar B, Ozer N, Gazioglu C (2011) Revision of the tsunami catalogue affecting turkish coasts and surrounding regions. Nat Hazards Earth Syst Sci 11:273–291. doi:10.5194/nhess-11-273-2011

Ayca A (2012) Development of a Web GIS-based tsunami inundation mapping service; a case study for Marmara Sea Region, Master of Science Thesis, METU, Department of Civil Engineering, Ocean Engineering Research Center, Ankara, Turkey

Aydın DI (2014) Tsunamis generated by submarine landslides in the Marmara Sea, Master of Science Thesis, Boğaziçi University, Kandilli Observatory and Earthquake Research Institute, Istanbul, Turkey

Aytore B (2015) Assessment of tsunami resilience of ports by high resolution numerical modeling: a case study for Haydarpaşa port in the Sea of Marmara, Master of Science Thesis, METU, Department of Civil Engineering, Ocean Engineering Research Center, Ankara, Turkey

Aytore B, Acar S, Yalciner AC, Zaytsev A (2013) Assessment of tsunami resilience of ports by high resolution numerical modeling; a case study for Haydarpaşa port in the Sea of Marmara, Proceedings of 26th International Tsunami Symposium Gocek, Turkey, p 135

Aytore B, Cankaya ZC, Yalciner AC, Suzen ML, Zaytsev A (2014) High resolution data processing and tsunami assessment and applications to ports in the Sea of Marmara. In Mega Earthquakes and Tsunamis in Subduction Zones–Forecasting Approaches and Implications for Hazard Assessment Rhodes Isl., Greece, p 19

GEBCO (2016) The general bathymetric chart of the Oceans, http://www.gebco.net/. Accessed Mar 2016

Guler HG, Arikawa T, Oei T, Yalciner AC (2015) Performance of rubble mound breakwaters under tsunami attack, a case study: Haydarpaşa port. Istanbul, Turkey

Hébert H, Schindelé F, Altinok Y, Alpar B, Gazioglu C (2005) Tsunami hazard in the Marmara Sea (Turkey): a numerical approach to discuss active faulting and impact on the istanbul coastal areas. Mar Geol 215(1–2):23–43. doi:10.1016/j.margeo.2004.11.006

Insel, I. (2009). The effects of the material density and dimensions of the landslide on the generated tsunamis, Master of Science Thesis, METU, Department of Civil Engineering, Ocean Engineering Research Center, Ankara, Turkey

Istanbul Metropolitan Municipality (2009), Population and Demographic Structure. http://www.ibb.gov.tr/sites/ks/en-US/0-Exploring-The-City/Location/Pages/PopulationandDemographicStructure.aspx. Retrieved 25 Dec 2014

NAMI DANCE Software (2016) http://namidance.ce.metu.edu.tr/pdf/NAMIDANCE-version-5-9-manual.pdf

Okada Y (1985) Surface deformation due to shear and tensile faults in a half-space. Bull Seismol Soc Am 75(4):1135–1154

OYO, IMM (2007). Simulation and Vulnerability Analysis of Tsunamis Affecting the Istanbul Coasts, Project report performed for Istanbul Metropolitan Municipality by Oyo Int. Co, Japan

Ozdemir KK (2014) Database development for tsunami information system. Master of Science Thesis, METU, Department of Civil Engineering, Ocean Engineering Research Center, Ankara, Turkey

Ozel N, Ocal N, Yalciner AC, Kalafat D, Erdik M (2011) Tsunami Hazard in the Eastern Mediterranean and Its Connected Seas: Toward a Tsunami Warning Center in Turkey. Soil Dyn Earthq Eng 31:598–610

Papadopoulos GA, Gracia E, Urgeles R, Sallares V, De Martini PM, Pantosti D, Gonzalez M, Yalciner AC, Mascle J, Sakellariou D, Salamon A, Tinti S, Karastathis V, Fokaefs A, Camerlenghi A, Novikova T, Papageorgiou A (2014) Historical and pre-historical tsunamis in the mediterranean and its connected seas: geological signatures, generation mechanisms and coastal impacts. Mar Geol 354:81–103. doi:10.1016/j.margeo.2014.04.014

Ünlü S (2007) Comparative analytical data in the source determination of unknown spilled oil in the Haydarpaşa Port (Marmara Sea), Turkey. Bull Environ Contam Toxicol 78(5):363–367. doi:10.1007/s00128-007-9199-2

Yalciner AC, Alpar B, Altınok Y, Özbay İ, Imamura F (2002) Tsunamis in the Sea of Marmara: historical documents for the past, models for the future. Mar Geol 190:445–463. doi:10.1016/S0025-3227(02)00358-4